

## NON-IDEAL I-V-CHARACTERISTICS OF BLOCK-CAST SILICON SOLAR CELLS

O. Breitenstein and J. Heydenreich

Max-Planck-Institute of Microstructure Physics, Weinberg 2, D-06120 Halle/S., Germany

**Keywords:** I-V-Characteristics, Shunt Resistance, Precipitation, Surface Currents, Surface Passivation

**Abstract.** A systematic investigation of cleaved pieces of solar cells of different sizes has lead to the conclusion that for pieces below 100 mm<sup>2</sup> the surface current dominates the I-V-characteristics. Reliable correlations between the defect content and the I-V-characteristics of small solar cell regions can be obtained using guarded mesa diode structures. The large n-factor of complete solar cells suggests that their forward current might be dominated by injection into charged interface layers. A theoretical description of this mechanism is presented, which allows also the interpretation of n-factors above n = 2.

### Introduction

The forward I-V-characteristics of a solar cell strongly influences its open-circuit voltage, its fill factor, and thus its efficiency. In normal operation solar cells are forward-biased, and the photogenerated current can be thought to be split into two parts; one being lead off and the other being internally back-injected. The relation of these two parts is bias-dependent and depends on the forward characteristics. Therefore, the study of the I-V-characteristics of solar cells is important for maximizing their efficiency. Especially, owing to the strong inhomogeneity of the electronic properties of large-grain polycrystalline silicon, the investigation of small solar cell regions and the correlation of their I-V-characteristics to the defect content in these regions should be a suitable tool to identify the factors being responsible for the deterioration of the I-V-characteristics of the whole solar cell. Classical diffusion theory leads to the well-known expression for the diffusion current of an n<sup>+</sup>p-junction [1]

$$j = \frac{I}{A} = \frac{D_n n_i^2}{L_d (N_A - N_D)} \left( \exp\left(\frac{eV}{kT}\right) - 1 \right) \quad (1)$$

(j: current density, I: current, A: diode area, D<sub>n</sub>: diffusion constant of electrons in the p-region, n<sub>i</sub>: intrinsic carrier concentration, L<sub>d</sub>: diffusion length within the p-region, (N<sub>A</sub> - N<sub>D</sub>): net doping concentration within the p-region, e: elementary charge, V: bias, kT: thermal energy). If recombination takes place via deep levels within the space charge region, the characteristics of diode currents are generally described by the relation

$$j = j_0 \left( \exp\left(\frac{eV}{n kT}\right) - 1 \right) \quad (2)$$

with n being the so-called n-factor and j<sub>0</sub> being a measure of the absolute reverse current density value. According to the Shockley-Read-Hall (SRH) theory [2] the n-factor can be in the range of 1 < n < 2; n-factors above n = 2 can not be explained within the framework of recombination via deep levels in the space charge region.

In the following I-V-measurements are presented that are directed to clarify the nature of the forward current flowing in solar cells. The results are discussed and a sample preparation technique is proposed allowing reliable I-V-measurements of small solar cell regions. A theoretical description of the current injection mechanism into charged interface layers is proposed, and the influence of impurities on the I-V-characteristics is discussed.

### Experimental

Readily processed  $n^+p$ -junction solar cells made from large-grain polycrystalline block-casted silicon (SILSO, Wacker-Chemitronic) have been investigated. The substrate net doping was  $(N_A - N_D) = 10^{16} \text{ cm}^{-3}$ . The cells have been divided into pieces of different sizes by diamond scratching from the backside and cleaving. I-V-characteristics have been measured and evaluated using a computer-controlled setup based on a KEITHLEY DAS-20 analog/digital interface card and a Burr-Brown LOG 100 JP logarithmic amplifier. The measurement and evaluation software was written based on the KEITHLEY VIEWDAC data acquisition and instrument control software running on an IBM 386 DX computer. EBIC-investigations have been carried out on a JEOL JSM 840A scanning electron microscope, and the IR-absorption measurements have been made using a Bruker IFS 66v FTIR spectrometer being equipped with an Oxford Instruments liquid helium cryostat.

### Results

Fig. 1: Forward I-V-characteristics measured at room temperature for a large ( $450 \text{ mm}^2$ , a) and a small ( $1.5 \text{ mm}^2$ , b) piece of a solar cell, for a solar cell mesa diode with (c) and without grain boundaries (d), and for a monocrystalline  $n^+p$ -junction (e; base-emitter junction of a pnp-transistor).

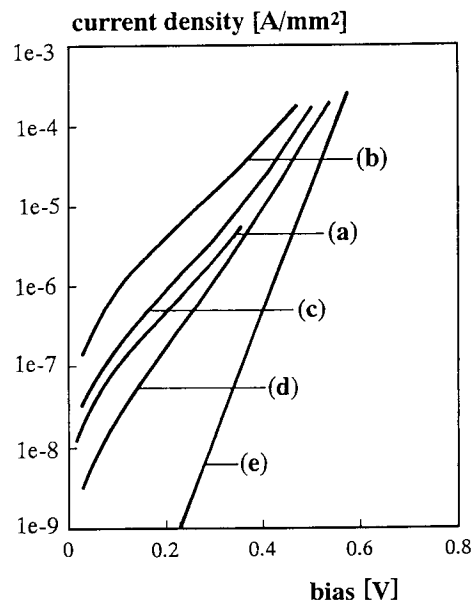


Fig. 1 shows forward I-V-characteristics of a large-area solar cell piece ( $A = 450 \text{ mm}^2$ ), of a small-area solar cell piece ( $A = 1.5 \text{ mm}^2$ ), of two solar cell mesa diodes (see below), and of a monocrystalline  $n^+p$ -junction (base-collector junction of a pnp-transistor,  $A = 0.25 \text{ mm}^2$ ), having the same net doping concentration of the p-region ( $10^{16} \text{ cm}^{-3}$ ) as the solar cells. Current densities are plotted so that the characteristics can be directly compared. While the n-factor of the monocrystalline junction was close to one, the solar cell samples showed a generally higher current density both in forward and in reverse direction. The solar cell pieces showed fairly straight exponential forward characteristics with n-factors of 2.5 and 2.6, respectively, well above  $n \leq 2$  as predicted by SRH recombination theory. The reverse characteristics of all solar cell samples were found to be fairly

ohmical rather than of saturation type, also in contrast to conventional diode theory. Though there was a unique correlation between the magnitude of the forward and the reverse currents of the different samples, owing to the good exponentiality over a wide bias range, the solar cell forward characteristics cannot be described as an ideal characteristic shunted by an ohmic resistance, as sometimes assumed. Instead, one has to look for an injection mechanism leading to  $n$ -factors above  $n = 2$ .

The difference between the large and the small solar cell piece (a) and (b) suggests that a surface current flows via the cleaved edges across the circumference of the solar cell pieces. A systematic investigation of a large number of solar cell pieces ranging from  $A = 1.5 \text{ mm}^2$  to  $A = 900 \text{ mm}^2$  showed that for  $A > 100 \text{ mm}^2$  both the forward and the reverse current are proportional to  $A$ , but for  $A < 100 \text{ mm}^2$  both are proportional to the circumference of the samples. Hence, for small solar cell pieces the dominating current is a surface current, and a reliable correlation of the I-V-characteristics to the defect content is not possible.

The most interesting result of this investigation was that the *shape* of the I-V-characteristics does not significantly change at the junction between volume-dominated and surface-dominated current. Hence, in spite of some scatter of the data due to inhomogeneities of the material, the  $n$ -factor was both for  $A < 100 \text{ mm}^2$  and for  $A > 100 \text{ mm}^2$  in the range  $2.3 < n < 2.9$ , and the reverse characteristics were ohmical. The conclusion is that the volume current of these solar cells should be governed by the same mechanism being responsible for surface currents across unpassivated surfaces of p-type silicon.

The passivation of p-silicon surfaces is an old and well-known problem in semiconductor technology. There are two main factors governing the surface charge, which are surface- or interface states and the fixed charge of oxide layers. The fixed oxide charge is known to be of positive sign, it is located immediately adjacent to the Si-SiO<sub>2</sub>-interface (hence it exists also for extremely thin oxide layers), and its magnitude is the higher the lower the oxidation temperature is [3]. Also interface states may trap positive charges from the p-material, so both factors may lead to a surface band bending into depletion or even into inversion, which is the reason for the surface currents appearing across free or oxidized p-silicon surfaces (see next section). The above result suggests that also the volume current flowing in our solar cell samples might be dominated by potential barriers of internal charged interfaces such as grain boundaries and/or dislocations penetrating the pn-junction.

It has been found that guarded mesa-diodes provide better suitable structures to measure the I-V-characteristics of small-area solar cell regions. The diodes have been prepared by masking the diode area and a closed ring-shaped "guard"-area around by a suitable resist, and etching a circular "ring" 100-200  $\mu\text{m}$  wide between both regions using a HF/HNO<sub>3</sub>-mixture to a depth of  $\approx 5 \mu\text{m}$ , well above the pn-junction depth of  $\approx 1 \mu\text{m}$ . For the measurement a bias is applied to the base contact, the guard-ring is grounded, and the diode current is measured against ground. Thus, no bias is applied across the unpassivated p-silicon surface gap between mesa-diode and guard-ring. Actually, both  $n^+$ -regions (diode and guard ring) are equally biased against the p-substrate and inject into the surface layer of the gap in between from both sides. These two currents cancel out if SRH recombination at the surface of the gap can be neglected, otherwise an additional SRH recombination current with  $1 < n < 2$  has to be expected. In Fig 1 (c) and (d) present two characteristics of  $A = 1.5 \text{ mm}^2$ -sized guarded mesa diodes, one of it containing electrically active grain boundaries (c), and the other one being positioned totally within one large grain (d), as investigated by light-microscopic and SEM/EBIC-observations. While the forward current density of the sample containing grain boundaries (c) clearly exceeds that of the large solar cell average (a), that of the other mesa (d) lies below. Thus, the mesa diodes show significantly lower currents than cleaved pieces of solar cells, and there is a correlation between the characteristics and the defect content that couldn't be found before. The  $n$ -factors are with  $n = 2.11$  (c) and  $n = 1.83$  (d) below that of the solar cell pieces ( $n \approx 2.6$ ). It can be assumed that the above mentioned SRH recombination at the depleted p-surface of the  $\approx 150 \mu\text{m}$  wide gap between the mesa diode and the guard-ring is still responsible for some part of this current. Further reduction of this gap width would further reduce this contribution.

### Theoretical description of current injection into an interface potential barrier

Fig. 2: Potential distribution at a charged interface (in front) crossing an  $n^+p$ -junction.  $E_c$ : conduction band edge,  $E_v$ : valence band edge,  $E_b$ : barrier height.

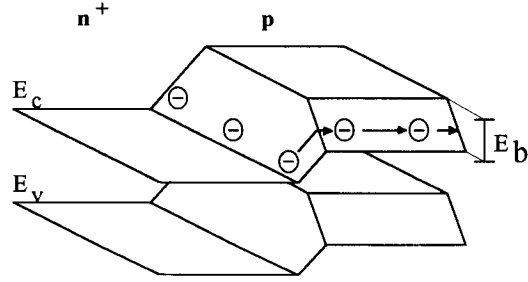


Fig. 2 shows schematically the potential distribution of an  $n^+p$ -junction at a charged surface or interface, respectively. Due to the interface charge density  $Q_i$  there is a barrier of the height  $E_b$  on the p-side of the interface. For zero bias these values should be  $Q_i^0$  and  $E_b^0$ .  $Q_i$  contains both interface-trapped and fixed charges. The interface should have an trap density of interface states  $N_{is}$ , being assumed to be energetically constant distributed in first approximation. The Fermi level crossing point at the interface (measured from the valence band edge there) should be  $\xi_i^0$  for zero bias. If a forward bias is applied to the diode, electrons are injected into the potential groove as shown in Fig. 2, hence at the interface the Fermi level splits into two quasi Fermi levels  $\xi_i^n$  and  $\xi_i^p$  which are differing by the applied bias:

$$\xi_i^n - \xi_i^p = eV \quad (3)$$

Thereby also the interface state charge diminishes by electron trapping, leading to a bias-dependent reduction of the interface barrier  $E_b$ . Assuming that the interface states are totally filled with electrons below  $\xi_i^p$  and totally empty above  $\xi_i^n$ , and that their average filling state between  $\xi_i^n$  and  $\xi_i^p$  is  $m$  ( $0 < m < 1$ ), depending on the capture cross sections to electrons and holes, using Eq. (3) the surface charge density can be written as:

$$Q_i = Q_i^0 - N_{is}(\xi_i^p - \xi_i^0 + m eV) \quad (4)$$

Since for nondegeneracy the p- Fermi level can be assumed to cross straight through the interface of the p-region at the junction, the shift of  $\xi_i^p$  equals the shift of the barrier height, hence

$$\xi_i^p - \xi_i^0 = E_b - E_b^0 \quad (5)$$

leading to

$$Q_i = Q_i^0 - N_{is}(E_b - E_b^0 + m eV) \quad (6)$$

Due to the neutrality requirement the interface charge density is connected with the barrier height and the net doping by

$$Q_i = (N_A - N_D)W = \sqrt{\frac{2 \epsilon \epsilon_0 (N_A - N_D) E_b}{e}} \quad (7)$$

( $W$ : space charge width,  $\epsilon \epsilon_0$ : dielectric constant) with  $Q_i(E_b^0) = Q_i^0$ . The square root in Eq. (7) can be developed around  $E_b = E_b^0$ , leading to

$$Q_i = Q_i^0 \left( 1 + \frac{1}{2} \frac{E_b - E_b^0}{E_b^0} \right) \quad (8)$$

Combining Eqs. (6) and (8) leads to the dependence of the barrier height at the p-side of the n<sup>+</sup>p-junction on the forward bias:

$$E_b = E_b^0 - m eV \frac{2E_b^0 N_{is}}{Q_i^0 + 2E_b^0 N_{is}} \quad (9)$$

Hence, for  $N_{is} \rightarrow 0$  the surface barrier is unaffected by the bias, and for high  $N_{is}$  the barrier reduces proportional to the applied bias. Assuming nondegeneracy, the injection into the edge of a surface space charge layer can be shown to be equivalent to the injection into a square-shaped potential groove of depth  $E_b$  and width

$$d = \frac{W kT}{2 E_b} = \frac{kT}{2} \sqrt{\frac{2 \epsilon \epsilon_0}{e (N_A - N_D) E_b}} \quad (10)$$

In this groove the injection current can be described by Eq. (1) multiplied by a Boltzmann-factor  $\exp(E_b/kT)$ :

$$I = l d \frac{D_n n_i^2}{L_d (N_A - N_D)} \left( \exp\left(\frac{eV}{kT}\right) - 1 \right) \exp\left(\frac{E_b}{kT}\right) \quad (11)$$

( $l$ : contributing length of the interface). Using Eq. (9), for  $eV > kT$  this relation can be written as

$$I = l d j_0^{\text{diff}} \exp\left(\frac{E_b^0}{kT}\right) \exp\left(\frac{eV}{n kT}\right) \quad (12)$$

with the n-factor

$$n = \frac{Q_i^0 + 2 E_b^0 N_{is}}{Q_i^0 + 2 E_b^0 N_{is} (1 - m)} \quad (13)$$

and  $j_0^{\text{diff}}$  being the prefactor of the normal diffusion current density according to Eq. (1). It is obvious that the absolute current value strongly depends on  $E_b^0$  (hence on the interface charge density  $Q_i$ ), and that (depending on  $N_{is}$  and  $m$ ) the n-factor can take large values well above  $n=2$ . If  $N_{is}$  and/or  $m$  vary with the energy position, also s-shaped characteristics can be explained, which also frequently occurred in our I-V-measurements. Within this theory, the surface current being responsible for the difference between Fig. 1 (a) and (b) can be quantitatively fitted using  $j_0^{\text{diff}} = 3 \times 10^{-13} \text{ A/mm}^2$  obtained experimentally from Fig. 1 (e), and the parameters  $E_b = 0.656 \text{ eV}$ ,  $m = 0.8$ , and  $N_{is} = 6.6 \times 10^{11} \text{ cm}^{-2} \text{ eV}^{-1}$ .

### Summary and discussion

It has been shown that the correlation between crystal defects and the I-V-characteristics of n<sup>+</sup>p solar cells can only be investigated using guarded mesa diode structures; otherwise uncontrolled

surface currents flowing across the unpassivated p-surface would mask the characteristics obtained. From the similarity of the characteristics of these surface currents to the characteristics of large solar cells it can be concluded that also the volume current in solar cells might be dominated by injection into charged interface regions, as the unpassivated p-surface current is. A theoretical description of this current injection process has been presented, leading to possible n-factors of the characteristics well above  $n = 2$ .

It is still an open question whether or not oxygen might be precipitated on crystal defects in this material and contributes to their defect charge via the above mentioned fixed oxide charge. To our knowledge no direct evidence for oxygen precipitation at defects in this material is available. It has, however, been calculated by Jones et al. [4] using cluster calculations that at least atomic incorporation of oxygen into dislocation cores is energetically advantageous. There has also been some indirect indication of oxygen precipitation in solar cell silicon by Pivac [5], who has found a significant increase of the concentration of interstitially dissolved oxygen after annealing the material at 1250°C and subsequently quenching it. We have carried out a similar experiment with our SILSO material. Slices of 4 mm thickness were investigated by FTIR absorption at 4K to yield the interstitial oxygen concentration. Then the slices were sealed in quartz ampoules evacuated below  $10^{-6}$  Torr and annealed at 1200°C for 5h. After quenching to room temperature the FTIR measurements were repeated. The evaluation of the data using a Czochralski sample of known interstitial oxygen content as a standard, lead to an interstitial oxygen concentration of  $[O_i] = 4.4 \times 10^{15} \text{ cm}^{-3}$  for the as-grown material and  $[O_i] = 2.7 \times 10^{16} \text{ cm}^{-3}$  for the annealed sample. Hence, also here some part of the oxygen should have been in a precipitated state most probably associated with lattice defects, where it is not IR-active but may contribute to defect charges. If oxygen should play a dominant role in charging crystal defects, this effect should be less severe if  $p^+n$ -structures would be used for solar cells instead of the  $n^+p$ -structures hitherto used. Note, that one argument for choosing  $n^+p$ -junctions was the higher radiation-hardness of the p-material [6], which should be not important for terrestrial applications.

Another impurity that might enhance the potential barrier around crystal defects is phosphorus. Since the conductivity of solar-grade silicon is typically adjusted by compensation, the material contains always some phosphorus. Palm and Schimpf [Cologne University, unpublished] have found evidence by EPR investigations that phosphorus might tend to concentrate on grain boundaries of this material. Then its positive ion charge would increase the defect charge and its electrostatic barrier around. By C-V- and I-V-measurements across single grain boundaries Häßler, Pensl and Schulz [Erlangen University, unpublished] have found that the barrier height in ultra-pure polycrystalline silicon material, being not counterdoped with phosphorus, is significantly lower than that of usual solar-grade polysilicon. Though it cannot be excluded that also other impurities might affect the barrier height, this result is consistent with the assumption that phosphorus increases the barrier height around crystal defects in solar-grade polysilicon. Also this effect would not appear in  $p^+n$  solar cells.

This work was supported by the Bundesminister für Forschung und Technologie (BMFT) under contract No. 0329 107 H. The authors are indebted to E. Schroer and J. Sperling (Halle) for experimental cooperation and to U. Gösele (Halle) and A. Voigt (Erlangen) for valuable discussions.

#### References:

- [1] E. Spenke: *Elektronische Halbleiter*, (Springer, Berlin, 1965)
- [2] E. S. Yong: *Fundamentals of Semiconductor Devices*, (McGraw-Hill, New York, 1978)
- [3] P. Balk (ed.): *The Si-SiO<sub>2</sub> System*, (Elsevier, Amsterdam, 1988)
- [4] R. Jones, A. Umerski, P. Sitch, M. I. Heggie and S. Öberg, *phys. stat. sol. (a)* **138**, 369 (1993)
- [5] B. Pivac: In *Polycrystalline Semiconductors-Grain Boundaries and Interfaces*, ed. by H. J. Möller, H. P. Strunk and J. H. Werner, Springer Proc. in Physics Vol. 35 (Springer, Berlin, 1989), p.170
- [6] M. A. Green, *Semicond. Sci. Technol.* **8**, 1 (1993)

**Polycrystalline Semiconductors III**  
10.4028/www.scientific.net/SSP.37-38

**Non-Ideal I-V-Characteristics of Block-Cast Silicon Solar Cells**  
10.4028/www.scientific.net/SSP.37-38.139